World Academy of Science, Engineering and Technology
International Journal of Mechanical and Materials Engineering
Vol:12, No:4, 2018

Optimization of Slider Crank Mechanism Using Design of Experiments and Multi-Linear Regression

Galal Elkobrosy, Amr M. Abdelrazek, Bassuny M. Elsouhily, Mohamed E. Khidr

***Abstract*—**Crank shaft length, connecting rod length, crank angle, engine rpm, cylinder bore, mass of piston and compression ratio are the inputs that can control the performance of the slider crank mechanism and then its efficiency. Several combinations of these seven inputs are used and compared. The throughput engine torque predicted by the simulation is analyzed through two different regression models, with and without interaction terms, developed according to multi-linear regression using LU decomposition to solve system of algebraic equations. These models are validated. A regression model in seven inputs including their interaction terms lowered the polynomial degree from 3rd degree to 1st degree and suggested valid predictions and stable explanations.

***Keywords*—**Design of experiments, regression analysis, SI Engine, statistical modeling.

NOMENCLATURE

SCM	Slider crank mechanism
TDC	Top dead center
BDC	Bottom dead center
OHV	Over head valve
r^2	Coefficient of determination
Y	Experimental response
Y_r	Predicted response
LSM	Least square method

I. INTRODUCTION

DESIGN of experiments is a series of tests in which purposeful changes are made to the input variables of a system or process. The effects on response variables are measured in order to understand cause-and-effect relationships on the system.

Perceptions on the framework or process can prompt speculations about what influences the framework to work; however; trials of the sort portrayed above are required to show that these hypotheses are right. Design of experiments is widely applicable to both physical processes and computer simulation models. Design of experiments is a powerful tool for expanding the amount of data picked up from an investigation while limiting the amount of data to be gathered.

Abdul Samad and Zainol [1] studied ferulic acid production, several factors such as temperature, pH, agitation, water-to-substrate ratio, volume of inoculums, fermentation time, and type of co-culture can influence the use of co-culture for ferulic acid production from banana stem waste. Among the deciding factors, the primary factor of pH and the influence of temperature and fermentation time had the most grounded impact on the production of ferulic acid.

Pawlak et al. [2] used design of experiments approach to prepare a mathematical model for selective laser melting (SLM), a technology used to produce objects from a wide variety of materials. The group of materials handled in this innovation involves stainless steel, CoCr, titanium and aluminum alloys and is constantly extending to incorporate new materials. It was demonstrated that data on linear energy density and scan velocity are not adequate to depict the SLM procedure, and that it is important to give definite estimations of component parameters.

Psychological stress has for quite some time been a quiet executioner, debilitating ordinary physiological capacities and prompting to an assortment of diseased conditions. Full factorial design was utilized by Kala et al. [3] for the development and optimization of psychological stress model in mice by applying different stressors: slanted cage, restraint, no bedding, dirty bedding and isolation at two time duration levels of 30 and 60 min. The statistical data showed that a quadratic model was fitted to the data obtained and all factors were found to have a significant role.

Turboelectric generators based on contact electrification and electrostatic induction have recently emerged as a promising mechanical energy harvesting technique. Making prediction of the output voltage of a turboelectric generator is a challenge. In addition, structural parameters such as area, gap and dielectric thickness, which affect the output voltage of the generator, have been investigated individually and with their interaction effects. Vasandani et al. [4] established two meta-models as a result of a 2^3 full factorial design. The models have been verified.

The applications of composite-metal stacks and fiber metal laminates (FMLs) are increasingly being used in aerospace structures due to their enhanced mechanical properties compared to composites or metals alone. During drilling of glass aluminum reinforced epoxy (GLARE) fiber-metal laminates: cutting forces, surface roughness, cutting tool

Galal Elkobrosy and Amr M. Abdelrazek are with the Engineering mathematics and physics Department-Faculty of Engineering – Alexandria University, Egypt.

Bassuny M. Elsouhily is with the Mechanical Engineering Department-Faculty of Engineering – Alexandria University, Egypt.

Mohamed E. Khidr is with the Engineering mathematics and physics Department-Faculty of Engineering – Alexandria University, Egypt (e-mail: memadkhidr@gmail.com).

condition and post-machining micro-hardness of the surface of the upper and lower aluminum sheets near the edge of drilled holes were investigated. Giasin et al. [5] used analysis of variance (ANOVA) to evaluate the impact of cutting parameters, and cooling conditions, and their percentage contributions when drilling GLARE.

In automotive technology field, there was an accelerated invention and innovation in suspension design. Mitra et al. [6] found the ideal combination of suspension and steering geometry parameters such as tire pressure, damping coefficient, spring stiffness, sprung mass, camber, toe and wheel speed, so that the Ride Comfort (RC) is increased while maintaining an optimal degree of Road Holding using Design of Experiments. The high R^2 value shows the high reliability and predictability of the experimental models.

D'Ambrosio and Ferrari [7] evaluated the potential of the after-injection versus engine-out emissions, combustion noise and brake specific fuel consumption for a Euro 5 diesel engine with a reduced compression ratio 16.3:1. Effects of injection strategies that feature either pilot and after-injection shots or double-pilot and single-after injection shots have been assessed experimentally in the presence of high EGR fractions. Calibrations with triple and quadruple injection schedules have been optimized by means of a design of experiments procedure. The experimental data refer to different steady-state working conditions that are representative of passenger car engine applications over the European homologation cycle.

Li et al. [8] used design of experiments and fractional factorial design to investigate the way that injection strategy might affect performance and emissions formation of reactivity controlled compression ignition engines RCCI. Six factors, namely the first start of injection (SOI) timing, the first injection duration (ID), the second SOI timing, the second ID, the diesel mass fraction in the first injection and the ratio of natural gas to total air, were considered. 16 simulated runs were conducted to evaluate the performance and emissions of an engine. The results show that premixed natural gas, which is the most dominant one, has a positive correlation with indicated power, and could reduce Carbon Monoxide (CO), Nitrogen Oxides (NOx) and soot emissions simultaneously. To further reduce NO_x, both retarded second SOI timing and extended second ID are suggested.

Tashtoush et al. [9] tested several bio-source-fuels like fresh and waste vegetable oil and waste animal fat at different injector pressures (120, 140, 190, 210 bar) in a direct-injection, naturally aspirated, single-cylinder diesel engine with a design injection pressure of 190 bar. Using factorial analysis, the effect of injection pressure (Pi) and fuel type on three engine parameters, namely, combustion efficiency (Zc), mass fuel consumption (m_f) and engine speed (N) was examined. It was found that Pi and fuel type significantly affected both Zc and m_f, while they had a slight effect on engine speed.

Da Silva. et al. [10] measured the behavior of the burrs' geometries generated in nine different positions of the edge of the work piece during face milling of motor engine blocks, varying thus the tool exit angle. During the tests the cutting speed, the feed rate, the depth of cut and the flank wear were varied. The wear and the tool exit angle had significant influences on the burr size. The greater the flank wear and the exit angle, the bigger the burr. The burr sizes were reduced with increasing the feed rate and in some cases with the depth of cut, but increases when the cutting speed was enhanced.

Trezona et al. [11] carried out a full factorial experimental investigation into factors affecting the resistance of a commercial acrylic/melamine automotive clear coat to erosion by silica sand particles. The factor variables and their ranges were: particle size, temperature, impact angle, particle velocity and the baking process applied to the coating. A linear regression model with r^2=97.5% was generated to evaluate the erosion response of the coating. The regression coefficients of this model evaluate the strengths of the impacts of every one of the variables. Interactions between the factors were distinguished. Specifically, the glass transition of the coating, which happens at 40°C, has a noteworthy impact on its response to erosion. The study has permitted the combinations of conditions that would be of most worry for car paint clients to be recognized.

In the prediction of the hydrodynamics of a liquid–solid circulating fluidized bed, Palkar and Shilapuram [12] studied the effects of the interactions among the independent factors considered on the performance variables. Different statistical models, for example the linear, two-factor association, quadratic and cubic models are tried. The model has been created to foresee reactions for example average solids holdup and solids circulation rate. The authenticity of the created regression model is checked utilizing the analysis of variance. Besides, the model created was contrasted with a test dataset to survey its competence and accuracy.

The use of daylight in buildings to save energy while providing satisfactory environmental comfort has increased. Integration of the day lighting and thermal energy systems is necessary for environmental comfort and energy efficiency. Kim et al. [13] developed an integrated model for a day lighting, heating, ventilating and air conditioning (IDHVAC) system to predict building energy performance by artificial lighting regression models. The design of experiments (DOE) method was applied to generate the database that was used to train robust model without over fitting problems. The IDHVAC system was optimized using the integrated model to minimize total energy consumption while satisfying both thermal and visual comfort for occupants.

Dong and Sartaj [14] investigated an application of microwave (MW) radiation followed by aeration for the purpose of ammonia removal from both synthetic solutions and landfill leachate. 100 mL of synthetic solution or landfill leachate was subjected to MW radiation for 30, 45, 60, 90 and 120 s under 50 and 100% power output level and a pH of 10, 10.5 and 11. The samples were then aerated for 10 min. The initial, after MW application and final total ammonia nitrogen (TAN) were measured. Design of experiments and factorial design were applied to evaluate and optimize the effects of pH, MW energy level and microwave power output. Results confirmed that the sequential microwave/aeration process was an effective approach for removal of ammonia from aqueous

systems. r^2 of 0.941 indicates that the observed results fitted well with the model prediction.

The system of edges sealing of vacuum glass boards is being used in an assortment of manufacturing applications for example in displays and home apparatuses. The sealing states of a vacuum glass board firmly influence its key execution parameters such as its isolation and intensity. Kim and Jeon [15] established a regression models for estimating the edge thickness, deflection, and maximum radius of the sealed part, which were considered as shape parameters. Four parameters; gas flow rate, torch movement speed, distance between the torch and the glass panels and the torch nozzle angled were selected as process parameters for the edge sealing process. The impacts of the procedure parameters on the shape parameters and in addition the interactions between them were tested, and a polynomial regression model that considered these interactions was set up. The plausibility of all the regression models was confirmed through analysis of variance.

Njoyaa and Hajjaji [16] investigated the changes in microstructure and technical properties of vitrified ceramic samples, prepared from kaolinitic-clay and feldspar-rich raw materials from Cameroon, against feldspar content, firing temperature and soaking time by X-ray diffraction and scanning electron microscope, and using full factorial design. The advancement of the two previous stages enhanced the studied ceramic properties. The consequences of the full factorial design demonstrated that temperature was the most effective variable, and its rise positively affected ceramic properties. The impacts of the flux content and soaking time were to some degree equivalent and their effects were like that of temperature. The impacts of interactions between the variables were moderately less essential and their weights contrasted for properties.

Controlling process parameters of lost foam casting (LFC) enables this process to produce defect-free complex shape castings. Jafari et al. [17] carried out an experimental investigation on lost foam casting of an Al−Si−Cu cast alloy. The impacts of pouring temperature, slurry viscosity, shaking time and sand size on surface finish, shrinkage porosity and eutectic silicon interval of thin-wall molding were inspected. A full two-level factorial design of empirical strategy was utilized to distinguish the huge manufacturing factors influencing the properties of casting. Pouring temperature was found as the most critical factor influencing Al−Si−Cu lost foam casting quality. It was shown that flask vibration time interacted with pouring temperature influenced eutectic silicon spacing and porosity percentage significantly. Furthermore, variation in slurry viscosity showed no significant effect on the evaluated properties compared to other parameters.

Laser cladding is a complicated process controlled by most parameters such as laser beam, properties of matrix and powder and treatment status of base material. Zhang et al. [18] found that the best way to choose the working conditions cheaply and fast is to use the processing simulation after regression design based on the experimental results of 2Cr13 steel cladding with diode laser robotized system. The influence degrees of technological factors (laser power, laser scanning speed, defocusing amount and powder feeding rate) on the dimensions and hardness of laser clad layers were investigated.

Hydrogen is predicted to conduct a huge part in future energy systems. The proficient generation of hydrogen at the very least cost and in an environmentally adequate way is critical for the advancement of a hydrogen-including economy. An imperative part of economical advancement is limiting irreversibility. Hajjaji et al. [19] examined the impact of the reformer working temperature, pressure and steam to carbon proportion (S/C) on the procedure exergetic effectiveness. By using design of experiment a second order polynomial mathematical model has been obtained through correlating the exergetic efficiencies with the reformer operating parameters.

II. Slider Crank Mechanism (SCM)

Slider crank mechanism is one of the most useful mechanisms in the present day application for internal combustion engines and numerous other applications such as robotics, pumps and compressors. SCM is a modification of four bar chain. It consists of one sliding pair and three turning pairs, see Fig. 1.

The SCM usually found in Reciprocating Steam engine mechanism and used to convert rotary motion to reciprocating motion and vice versa. However, when it is used in automobile engine, it converts the available energy (force on the piston) to the desired energy (torque of the Crank shaft) which is used to move a vehicle.

Reciprocating pumps, reciprocating compressors, and steam engines are other examples of machines derived from the slider crank mechanism.

KOHLER Engine CH270: is a spark ignition engine with four strokes, single cylinder design with a cast iron cylinder bore and overhead valve for easy access.

TABLE I
Specifications of the KOHLER Engine CH270

4 Stroke, Gasoline, OHV Cast iron cylinder liners, Aluminum block		
Rated Power	(hp / kW)	7 / 5.2
Displacement	(cc)	208
Bore	(mm)	70
Stroke	(mm)	54
Crank radius	(mm)	27
Compression Ratio		8.5:1
Lubrication		Splash
Rated Speed	(RPM)	4000

The working cycle is completed after four strokes of the piston or two revolutions of the crank shaft. This achieved by carrying out suction, compression, power and exhaust processes in each stroke, see Figs. 2 and 3.

1) Intake: It is also known as induction or suction which begins at TDC and ends at BDC. The intake valve must be in the open position while the piston pulls an air-fuel mixture into the cylinder by producing vacuum pressure into the cylinder through its downward motion.
2) Compression: This stroke begins at BDC or just at the end of the suction stroke and ends at TDC. The piston

compresses the air-fuel mixture in preparation for ignition during the power stroke. Both the intake and exhaust valves are closed during this stage.

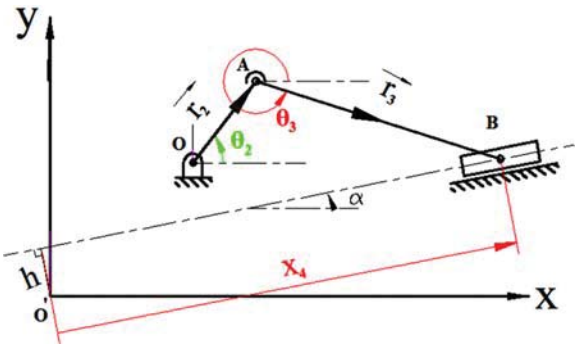

Fig. 1 Schematic representation of slider crank mechanism

3) Combustion: It is also known as power or ignition which starts at the second revolution of the four stroke cycle, at this point the crankshaft has completed a full 360-degree revolution. While the piston is at TDC, the compressed air-fuel mixture is ignited by a plug, forcefully returning the piston to BDC.
4) Exhaust: During the exhaust stroke, the piston once again returns from BDC to TDC while the exhaust valve is open. This action expels the spent air-fuel mixture through the exhaust valve.

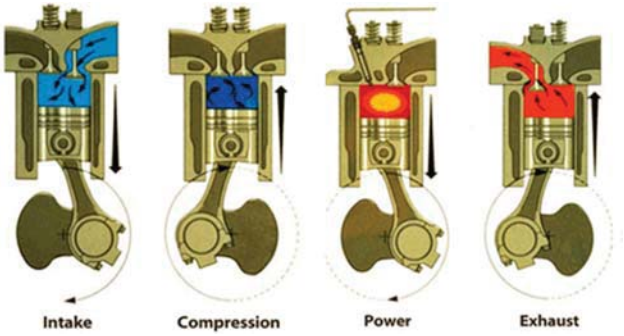

Fig. 2 Four strokes cycle

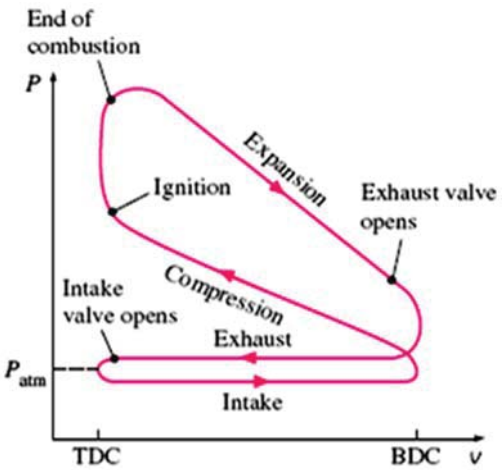

Fig. 3 Pressure-volume diagram for 4-stroke spark ignition engine

III. Statistical Design of Experiments

Regression analysis allows the simultaneous study of the effects that several factors may have on the optimization of a particular process. It determines which factors have the important effects on the response as well as how the effect of one factor varies with the level of the other factors. The effects are the differential quantities expressing how a response changes as the levels of one or more factors are changed.

Regression analysis allows measuring the interaction between each different group of factors. The interactions are the driving force in many optimizations of the processes. Without the use of Regression analysis, some important interactions may remain undetected, and the overall optimization may not be attained.

In this investigation, seven operating factors were chosen as independent variables, namely: Crank angle (x_1), Engine RPM (x_2), Compression ratio (x_3), Crank shaft length (x_4), Connecting rod length (x_5), Cylinder bore (x_6) and Mass of piston (x_7). The natural values of each factor and their respective levels are shown in Table II.

TABLE II
The Experimental Ranges and Levels of Independent Variables

Factors			Levels	
Crank Angle	X_1	(Degree)	0°	180°
Engine Speed	X_2	(RPM)	1500	3500
Compression Ratio	X_3		6	12
Crank Shaft Length	X_4	(mm)	10	40
Connecting Rod Length	X_5	(mm)	60	110
Cylinder Bore	X_6	(mm)	50	100
Mass Of Piston	X_7	(g)	200	700

A dynamical analysis - Complete Position, Velocity, Acceleration and Force analysis - of single cylinder SI engine was conducted. Configuration of the engine to which the crankshaft belongs is shown in Table I. The equations which are used in MATLAB provided the values of angular velocity and angular acceleration of the crank shaft and pressure force at the piston tip. The advantage of using MATLAB programming is that any changes in the input could be made very easily and solution quickly obtained.

The design performed according to TABLE III was composed of 20 random runs to see the effect on the output engine torque Y to fit the following polynomial equation:

$$\mathbf{Y = b_0 + \sum_{i=1}^{k} b_i X_i + \varepsilon} \quad (1)$$

where Y is the estimated response of Engine torque; b_0 is the intercept of the plane; b_i is the linear and interaction term effects.

A regression analysis is carried out to determine the coefficients of the response model b_1, b_2, ….b_k, as well as their standard errors and their significance, in addition to the constant b_0 and error ε terms.

TABLE III
RANDOM RUNS OF SLIDER CRANK MECHANISM FORCE ANALYSIS

Run no.	X_1	X_2	X_3	X_4	X_5	X_6	X_7	Y
1	148	2400	11.4	0.022	0.099	0.07	0.61	117.949
2	136	2200	7.3	0.034	0.108	0.066	0.54	111.1763
3	79	3200	10.6	0.015	0.103	0.1	0.46	245.8034
4	159	2700	6.9	0.016	0.08	0.088	0.62	46.62158
5	142	2100	9.2	0.012	0.065	0.056	0.54	35.26573
6	89	1800	9	0.014	0.062	0.093	0.48	166.1124
7	167	2900	9.5	0.035	0.104	0.1	0.2	149.1107
8	155	2700	12	0.026	0.084	0.09	0.31	221.1714
9	90	3300	9.5	0.036	0.097	0.079	0.32	309.6958
10	120	1600	9.8	0.03	0.097	0.095	0.7	407.7961
11	138	2700	11.6	0.027	0.06	0.056	0.63	119.0929
12	87	3200	7.2	0.027	0.092	0.051	0.51	59.85134
13	65	1600	8.9	0.015	0.066	0.06	0.27	60.947
14	34	1500	9.8	0.018	0.087	0.085	0.45	94.90406
15	96	2400	6.7	0.025	0.103	0.094	0.33	206.9902
16	38	2600	9.9	0.022	0.07	0.098	0.24	158.2207
17	19	1700	7	0.029	0.089	0.052	0.67	23.165
18	131	3000	6.3	0.036	0.107	0.1	0.63	232.7235
19	141	2500	7	0.022	0.066	0.051	0.67	30.32325
20	54	2100	8	0.024	0.093	0.051	0.62	57.70045

IV. RESULTS AND DISCUSSION

The model equation for engine torque was obtained after performing twenty runs and discarding the insignificant effects using some statistical tests to obtain r^2 which provides a measure of how well observed outcomes are replicated by the model, based on the proportion of total variation of outcomes explained by the model.

Regression coefficients were estimated by least square method (LSM) techniques using LU-Decomposition to solve system of algebraic equations. The results obtained shown in Tables IV-VII. Starting with first order model, TABLE IV represents the coefficients of the response model.

TABLE IV
COEFFICIENTS OF THE RESPONSE MODEL IN 1ST ORDER POLYNOMIAL EQUATION $R^2 = 0.68928$

Factors	Coefficient	Factors	Coefficient
b_0	-496.7619	X_4	5331.1316
X_1	-0.2597	X_5	175.5633
X_2	$-4.95x10^{-5}$	X_6	3573.5383
X_3	20.0506	X_7	142.7104

A comparison between the experimental data and the model obtained from first order polynomial equation (2) presented in Fig. 4.

$$\mathbf{Y_r = -496.7619 - 0.2597\,X_1 - 4.95x10^{-5}\,X_2 + 20.0506\,X_3 + 5331.1316\,X_4 + 175.5633\,X_5 + 3573.5383\,X_6 + 142.7104\,X_7} \quad (2)$$

In first order polynomial, r^2 was about 0.68928 and it is clear from Fig. 4 that the model obtained cannot capture the experimental results, so a second order polynomial model was introduced in Table V.

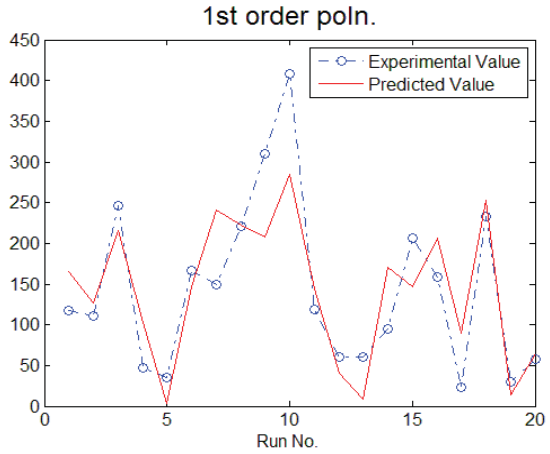

Fig. 4 Analysis of quality of 1st order model: comparison between experimental and predicted responses

TABLE V
COEFFICIENTS OF THE RESPONSE MODEL IN 2ND ORDER POLYNOMIAL EQUATION $R^2 = 0.9621$

Factors	Coefficient	Factors	Coefficient
b_0	- 1139.659	X_1^2	-0.0402
X_1	7.4983	X_2^2	$-1.87x10^{-5}$
X_2	0.0614	X_3^2	3.5534
X_3	-39.2918	X_4^2	436143.5626
X_4	-15473.9663	X_5^2	-157418.764
X_5	26585.4824	X_6^2	5751.9921
X_6	2351.9549	X_7^2	1187.5795
X_7	-969.5481		

By using the same data in TABLE III and by using least square techniques and LU-Decomposition to solve system of equations, the results obtained from second order model are shown in (3).

$$\mathbf{Y_r = -1139.659 + 7.4983\,X_1 + 0.0614\,X_2 - 39.2918\,X_3 -}$$

$$15473.9663\,X_4 + 26585.4824\,X_5 + 2351.9549\,X_6 - 969.5481\,X_7 - 0.0402\,X_1^2 - 1.87x10^{-5}X_2^2 + 3.5534\,X_3^2 + 436143.5626\,X_4^2 - 157418.764\,X_5^2 + 5751.9921\,X_6^2 + 1187.5795\,X_7^2 \quad (3)$$

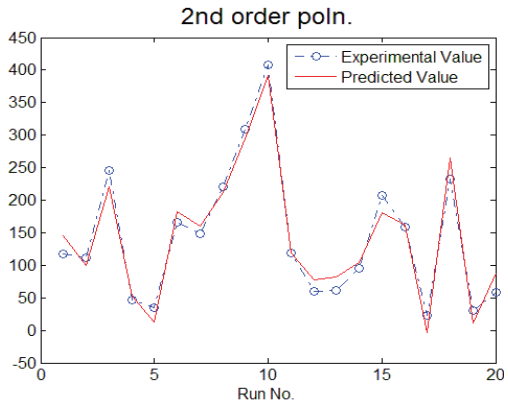

Fig. 5 Analysis of quality of 2nd order model: comparison between experimental and predicted responses

The correlation coefficient obtained for this model was 0.9621. Fig. 5 shows coincide between the experimental results and the model in many points. A polynomial from third order (4) is conducted by using least square techniques and solving the equations by using LU-Decomposition and the coefficients shown in TABLE VI.

TABLE VI
COEFFICIENTS OF THE RESPONSE MODEL IN 3RD ORDER POLYNOMIAL EQUATION $R^2 = 0.9975$

Factors	Coefficient	Factors	Coefficient
b_0	-997.8756	X_4^2	3240279.5729
X_1	2.9714	X_5^2	-55121.8337
X_2	-0.8371	X_6^2	406217.4986
X_3	419.0146	X_7^2	-13783.5895
X_4	-81660.6305	X_1^3	$-8.99x10^{-5}$
X_5	9239.5551	X_2^3	$-6.2x10^{-8}$
X_6	-25859.3023	X_3^3	1.2892
X_7	5480.6054	X_4^3	-38441627.4846
X_1^2	-0.0024	X_5^3	50931.3132
X_2^2	0.0004	X_6^3	-1850644.6887
X_3^2	-39.7317	X_7^3	10863.562

Substitute coefficients in equation we get:

$$Y_r = -997.8756 + 2.9714\,X_1 - 0.8371\,X_2 + 419.0146\,X_3 - 81660.6305\,X_4 + 9239.5551\,X_5 - 25859.3023\,X_6 + 5480.6054\,X_7 - 0.0024\,X_1^2 + 0.0004\,X_2^2 - 39.7317\,X_3^2 + 3240279.5729\,X_4^2 - 55121.8337\,X_5^2 + 406217.4986\,X_6^2 - 13783.5895\,X_7^2 - 8.99x10^{-5}\,X_1^3 - 6.2x10^{-8}X_2^3 + 1.2892\,X_3^3 - 38441627.4846\,X_4^3 + 50931.3132\,X_5^3 - 1850644.6887\,X_6^3 + 10863.562\,X_7^3 \quad (4)$$

Fig. 6 shows that the third order model is the most coincide with the experimental data and the coefficient of determination $r^2 = 0.9975$. We notice a similarity between the curves in most of points.

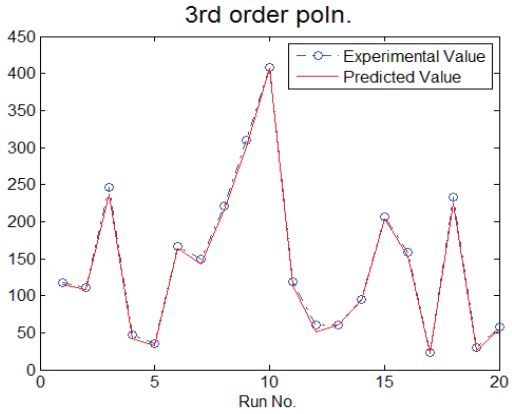

Fig. 6 Analysis of quality of 3rd order model: comparison between experimental and predicted responses

Using interaction between input variables:

$$Y_r = b_0 + \sum_{i=1}^{7} b_i X_i + \sum_{\substack{i=1 \\ j=2}}^{7} b_{ij} X_i X_j + \varepsilon \quad (5)$$

and solving system of equations obtained, we get the model coefficients shown in TABLE VII.

TABLE VII
COEFFICIENTS OF THE RESPONSE MODEL IN 1ST ORDER POLYNOMIAL EQUATION WITH INTERACTION TERMS $R^2 = 0.99992$

Factors	Coefficient	Factors	Coefficient
b_0	860.80306	X_2*X_4	5.2689
X_1	- 0.39613	X_2*X_5	3.59799
X_2	- 0.072	X_2*X_6	-0.11352
X_3	- 92.52979	X_2*X_7	-0.61657
X_4	7251.44271	X_3*X_4	-1010.15828
X_5	- 1967.21752	X_3*X_5	125.00625
X_6	- 3400.28652	X_3*X_6	404.99296
X_7	- 1028.9508	X_3*X_7	48.59408
X_1*X_2	- 0.00141	X_4*X_5	-76543.39541
X_1*X_3	0.42717	X_4*X_6	-146170.69637
X_1*X_4	138.21361	X_4*X_7	-1804.7426
X_1*X_5	- 134.6116	X_5*X_6	32381.17316
X_1*X_6	49.25636	X_5*X_7	11769.70331
X_1*X_7	10.50497	X_6*X_7	-814.0548
X_2*X_3	0.00155		

The equation obtained will be as follows and the coefficient of determination $r^2 = 0.99992$.

$$Y_r = 860.80306 - 0.39613\,X_1 - 0.072\,X_2 - 92.52979\,X_3 + 7251.44271\,X_4 - 1967.21752\,X_5 - 3400.28652\,X_6 - 1028.9508\,X_7 - 0.00141\,X_1X_2 + 0.42717\,X_1X_3 + 138.21361\,X_1X_4 - 134.6116\,X_1X_5 + 49.25636\,X_1X_6 + 10.50497\,X_1X_7 + 0.00155\,X_2X_3 + 5.2689\,X_2X_4 + 3.59799\,X_2X_5 - 0.11352\,X_2X_6 - 0.61657\,X_2X_7 - 1010.15828\,X_3X_4 + 125.00625\,X_3X_5 + 404.99296\,X_3X_6 + 48.59408\,X_3X_7 - 76543.39541\,X_4X_5 - 146170.69637\,X_4X_6 - 1804.7426\,X_4X_7 + 32381.17316\,X_5X_6 + 11769.70331\,X_5X_7 - 814.0548\,X_6X_7 \quad (6)$$

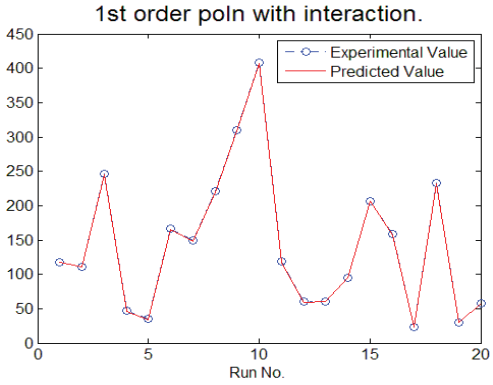

Fig. 7 Analysis of quality of 1st order interaction model: Comparison between experimental and predicted responses

Fig. 7 and r^2 indicate that the mathematical model is adequate and that there is consistency between the experimental and predicted values of the response. Also using equation from first ordaser with interaction terms gives better correlation from third order polynomial without interaction.

In the 3rd order model without interaction terms, connecting rod length X_5 has the strongest effect on the response since its coefficient $b_5 = 9239.5551$ is larger than the coefficients of the other investigated factors while in interaction model Crank Shaft Length X_4 has the strongest effect on the response b_4=7251.44271.

The negative sign b_4= - 81660.6305 in 3rd order model indicates that there is an inverse relation between crank shaft length X_4 and the response engine torque while the positive sign b_4 = 7251.44271 in interaction model indicates an opposite trend.

The most significance interactions found by the design of experiments are between crank shaft length $X_4$and cylinder bore X_6, b_{46}= - 146170.69637.

V. Conclusion

A regression model was developed according to multi-linear regression using LU decomposition to determine the main effects of crank shaft length, connecting rod length, crank angle, engine rpm, cylinder bore, mass of piston and compression ratio on engine torque. However, design of experiments did not provide the optimal conditions; it represented an understanding on the influence of several variables on the engine torque and their trends and behavior.

The polynomial degree lowered from 3rd degree to 1st degree when interaction terms were taken in consideration resulting in higher r^2.

The regression equation obtained shows that crank shaft length, connecting rod length and cylinder bore have an individual influence on the engine torque. The significance interactions found through the design of experiments between crank shaft length – cylinder bore X_4X_6 and between crank shaft length– connecting rod length X_4X_5.

References

[1] Abdul Samad. K., Zainol. N., The use of factorial design for ferulic acid production by co-culture: Industrial Crops and Products 95 (2017) 202–206.
[2] Pawlak. A., Rosienkiewicz. M., Chlebus. E., Design of experiments approach in AZ31 powder selective laser melting process optimization: Archives of Civil and Mechanical Engineering 17 (2017) 9–18.
[3] Kala. M., Shaikh. M. V., Nivsarkar. M., Development and optimization of psychological stress model in mice using 2 level full factorial design: Journal of Pharmacological and Toxicological Methods 82 (2016) 54–61.
[4] Vasandani. P., Mao. Z. H., Jia. W., Sun. M., Design of simulation experiments to predict turboelectric generator output using structural parameters: Simulation Modeling Practice and Theory 68 (2016) 95–107.
[5] Giasin. K., Soberanis. S.A., Hodzic. A., Evaluation of cryogenic cooling and minimum quantity lubrication effects on machining GLARE laminates using design of experiments: Journal of Cleaner Production 135 (2016) 533-548.
[6] Mitra. A. C., Kiranch and. G. R, Soni. T., Banerjee. N., Design of Experiments for Optimization of Automotive Suspension System Using Quarter Car Test Rig: Procedia Engineering 144 (2016) 1102–1109.
[7] D'Ambrosio. S., Ferrari. A., Potential of multiple injection strategies implementing the after shot and optimized with the design of experiments procedure to improve diesel engine emissions and performance: Applied Energy 155 (2015) 933–946.
[8] Li. J., Yang. W. M., Goh. T. N., An. H., Maghbouli. A., Study on RCCI (reactivity controlled compression ignition) engine by means of statistical experimental design: Energy 78 (2014) 777-787.
[9] Tashtoush. G. M., AlWidyan. M. I., Albatayneh. A. M., Factorial analysis of diesel engine performance using different types of biofuels: Journal of Environmental Management 84 (2007) 401–411.
[10] Da Silva. L. C., De Melo. A. C., Machado. L. R., Da Silva. M. B., Souza J´unior. A. M., Application of factorial design for studying the burr behavior during face milling of motor engine blocks. Journal of Materials Processing Technology 179 (2006) 154–160.
[11] Trezona. R. I., Pickles. M. J, Hutchings. I. M., A full factorial investigation of the erosion durability of automotive clear coats: Tribology International 33 (2000) 559–571.
[12] Palkar. R. R., Shilapuram. V., Detailed parametric design methodology for hydrodynamics of liquid–solid circulating fluidized bed using design of experiments: Particuology 31 (2017) 59–68.
[13] Kim. W., Jeon. Y., Kim. Y., Simulation-based optimization of an integrated day lighting and HVAC system using the design of experiments method: Applied Energy 162 (2016) 666–674.
[14] Dong. S., Sartaj. M., Statistical analysis and optimization of ammonia removal from landfill leachate by sequential microwave/aeration process using factorial design and response surface methodology: Journal of Environmental Chemical Engineering 4 (2016) 100–108.
[15] Kim. Y., Jeon. E. S., Establishment of regression model for estimating shape parameters for vacuum-sealed glass panel using design of experiments: Vacuum 121 (2015) 113-119.
[16] Njoya. D., Hajjaji. M., Quantification of the effects of manufacturing factors on ceramic properties using full factorial design: Journal of Asian Ceramic Societies 3 (2015) 32–37.
[17] Jafari. H., Idris. M. H., Shayganpour. A., Evaluation of significant manufacturing parameters in lost foam casting of thin-wall Al−Si−Cu alloy using full factorial design of experiment: Trans. Nonferrous Met. Soc. China 23(2013) 2843−2851.
[18] Zhang. Q., Anyakin. M., Zhuk. R., Pan. Y., Kovalenko. V., Yao. J., Application of Regression Designs for Simulation of Laser Cladding: Physics Procedia 39 (2012) 921–927.
[19] Hajjaji. N., Renaudin. V., Houas. A., Pons. M. N., Factorial design of experiment (DOE) for parametric exergetic investigation of a steam methane reforming process for hydrogen production. Chemical Engineering and Processing 49 (2010) 500–507.